Proceeding Paper

Early Results on GNSS Receiver Antenna Calibration System Development [†]

Antonio Tupek [1,*], Mladen Zrinjski [1], Marko Švaco [2] and Đuro Barković [3]

[1] Chair of Instrumental Technique, Faculty of Geodesy, University of Zagreb, Kačićeva 26, 10000 Zagreb, Croatia; mladen.zrinjski@geof.unizg.hr

[2] Department of Robotics and Production System Automation, Faculty of Mechanical Engineering and Naval Architecture, University of Zagreb, Ivana Lučića 5, 10000 Zagreb, Croatia; marko.svaco@fsb.hr

[3] Chair of Land Surveying, Faculty of Geodesy, University of Zagreb, Kačićeva 26, 10000 Zagreb, Croatia; djuro.barkovic@geof.unizg.hr

[*] Correspondence: antonio.tupek@geof.unizg.hr

[†] Presented at the 10th International Electronic Conference on Sensors and Applications (ECSA-10), 15–30 November 2023; Available online: https://ecsa-10.sciforum.net/.

Abstract: Precise Global Navigation Satellite Systems (GNSS) positioning is based on carrier phase observations where the understanding of receiver antenna's phase center corrections (PCCs) is critical. With the main goal of determining the PCC models of GNSS receiver antennas, only a few antenna calibration systems are in operation or under development worldwide. In this paper, the new automated GNSS receiver antenna calibration system, recently developed at the Laboratory for Measurements and Measuring Technique (LMMT) of the Faculty of Geodesy of the University of Zagreb in Croatia, is shortly presented. The developed system is an absolute field calibration system based on the utilization of a Mitsubishi MELFA RV-4FML-Q 6-axis industrial robot. The antenna PCC modelling is based on triple-difference carrier phase observations and spherical harmonics (SH) expansion. Our early calibration results, for the Global Positioning System (GPS) L1 frequency, show sub-millimeter agreement with the IGS approved Geo++ GmbH values.

Keywords: GNSS; antenna calibration; industrial robot; phase center correction (PCC)

1. Introduction

For high-accuracy global positioning applications on the centimeter and millimeter level, Global Navigation Satellite Systems (GNSS) receivers are essential sensors. To obtain the required accuracy level, all influential factors and error sources must be understood and, in an appropriate manner, accounted for. One such important influence is the phase center correction (PCC) of GNSS receiver antennas.

Because of the antenna's design characteristics and electromagnetic properties [1], the geometric location of GNSS signal reception, i.e., the antenna phase center (PC), is changing with respect to the incoming signal's direction and frequency [2–4]. Such variations cause advances and delays in carrier phase observations and corresponding range errors. Therefore, receiver antenna calibration is needed.

Today, *absolute filed calibration* is state-of-the-art when it comes to GNSS receiver antenna calibration. Only a few calibration systems utilizing a precise robot are operational or under development worldwide [5–12], and even fewer are accredited by the International GNSS Service (IGS) to provide antenna calibration results [13]. Since this topic is of high interest to the scientific antenna community, and a new calibration system is highly desirable, at the Laboratory for Measurements and Measuring Technique (LMMT) of the Faculty of Geodesy of the University of Zagreb in Croatia, a new antenna calibration system has been developed [14].

In this article preliminary antenna calibration results for the Global Positioning System (GPS) L1 frequency (G01) are presented and elaborated. Furthermore, the results on LMMT calibration validation with Geo++ GmbH are presented and discussed.

2. Materials and Methods

2.1. The Receiver Antenna Phase Center Correction Model

To fulfill the requirements of high-accuracy positioning applications, the receiver antenna PCCs must be determined. In line with the IGS convention, and as depicted in Figure 1, PCC is divided into the phase center offset (PCO) vector and the azimuth- and elevation-dependent phase center variation (PCV) [4,6,10–12,14]:

$$PCC\left(\alpha^i, z^i\right) = -\mathbf{e}^{\mathrm{T}}\left(\alpha^i, z^i\right) \cdot \mathbf{PCO} + PCV\left(\alpha^i, z^i\right) + r. \tag{1}$$

where $\mathbf{e}\left(\alpha^i, z^i\right)$ is the line-of-sight unit vector from the receiver to the satellite i and r is the constant part equal in all directions present due to the relative characteristics of GNSS measurements [4,6]. The PCO is a vector from the antenna reference point (ARP) to an arbitrarily defined mean phase center (MPC). The PCV is the direction-dependent range correction function, i.e., the difference between the real and ideal phase wavefront. The PCCs, and all corresponding antenna-related points, vectors, and scalars, are defined in an 3D antenna-fixed left-handed coordinate system (antenna frame–AF).
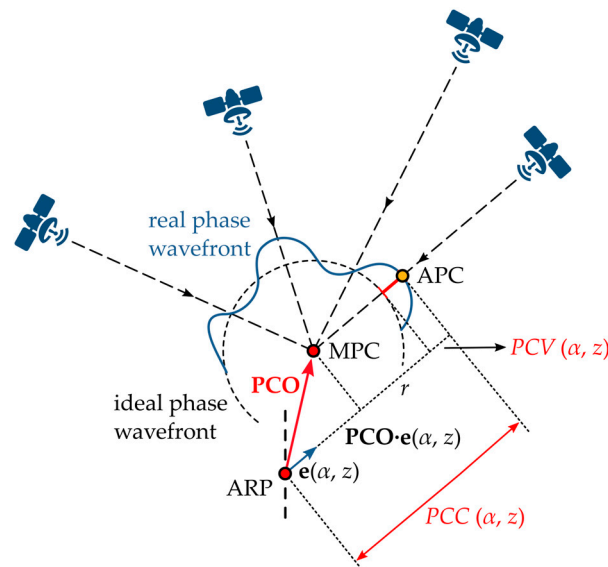
Figure 1. Definition and geometrical interpretation of the adopted GNSS receiver antenna phase center correction (PCC) model; ARP—Antenna Reference Point; MPC—Mean Phase Center; APC—Actual Phase Center; PCO—Phase Center Offset; PCV—Phase Center Variation.

A set of PCCs of an antenna are transformed to PCO and PCVs by a least squares (LSQ) adjustment and simultaneously fulfilling two conditions. Firstly, the PCV at antenna zenith are constrained to zero, i.e., zero-zenith constraint, by $PCV\left(\alpha^i, z^i = 0°\right) = 0$. Secondly, the PCO is determined as such that the sum of squared PCVs is minimal, i.e.,

$$\sum\left[PCV\left(\alpha^i, z^i\right)^2\right] \rightarrow \min.$$

2.2. Antenna Calibration Method at LMMT

To efficiently sample the entire antenna-under-test (AUT) hemisphere during calibration, at LMMT, a 6-axis industrial robot Mitsubishi MELFA RV-4FLM-Q is utilized. The robot turns the AUT in 2088 different antenna orientations, with stationary 2.5 s at every single orientation. Therefore, depending on the calibration timing parameters, a full calibration at LMMT lasts approx. 2 h. During calibration, a reference station (REF) on a 5-m short baseline is used. On both stations (REF and AUT) simultaneous 10 Hz raw carrier phase observations are registered with equal receiver settings. Afterwards, prior to PCC LSQ estimation, the carrier phase measurements are preprocessed to eliminate the majority of GNSS error sources.

Generally, the calibration system at LMMT is based on the triple-difference (TD) approach, i.e., time-differenced double-difference carrier phase observations [15]. A generic GNSS observation equation from receiver A to satellite *i*, in units of length, reads [16]:

$$\Phi_A^i = \rho_A^i + c\left(\delta t_A - \delta t^i + dt^{\mathrm{rel}}\right) + \xi_A^i + c\left(dt_A - dt^i\right) + T_A^i - I_A^i + \lambda N_A^i + \lambda \omega_A^i + MP_A^i + \varepsilon_A^i, \quad (2)$$

where ρ_A^i is the geometric distance, c the speed of light, δt_A and δt^i the receiver and satellite clock errors, dt^{rel} is the relativistic effects term, ξ_A^i is the combined satellite and receiver antennas PCC value, dt_A and dt^i the receiver and satellite hardware delays, T_A^i is the tropospheric delay, I_A^i is the ionospheric delay, λ is the signal wavelength, N_A^i is the integer phase ambiguity, ω_A^i is the carrier phase wind-up (PWU) effect, MP_A^i is the multipath term, and ε_A^i is the phase observation noise term.

Forming TD carrier phase observations needed for antenna calibration includes eight raw observations, from Equation (2), on the REF (R) and AUT (T) receiver for two satellites *i* and *j*, in two epochs t_k and t_{k+1}:

$$
\begin{aligned}
TD_{T,R}^{ij}\left(t_k, t_{k+1}\right) &= \Phi_R^j\left(t_{k+1}\right) - \Phi_T^j\left(t_{k+1}\right) - \Phi_R^i\left(t_{k+1}\right) + \Phi_T^i\left(t_{k+1}\right) - \Phi_R^j\left(t_k\right) + \Phi_T^j\left(t_k\right) + \Phi_R^i\left(t_k\right) - \Phi_T^i\left(t_k\right) \\
&= -PCC_T^j\left(t_{k+1}\right) + PCC_T^i\left(t_{k+1}\right) + PCC_T^j\left(t_k\right) - PCC_T^i\left(t_k\right) + \partial\varepsilon_{T,R}^{ij}.
\end{aligned} \quad (3)
$$

By exploiting the high spatial and temporal correlation of GNSS observations, and by forming TDs on a short baseline between two time-adjacent AUT orientations, the final TDs contain only the AUT PCCs and the differential phase noise $\partial\varepsilon_{T,R}^{ij}$. At LMMT, the PCCs are parametrized by spherical harmonic (SH) expansion with a degree and order resolution of $m = n = 8$ by:

$$PCC\left(\alpha^i, z^i\right) = \sum_{m=0}^{m_{\max}} \sum_{n=0}^{m} \tilde{P}_{mn}\left[\cos\left(z^i\right)\right] \cdot \left[a_{mn}\cos\left(n\alpha^i\right) + b_{mn}\cos\left(n\alpha^i\right)\right]. \quad (4)$$

where $\tilde{P}_{mn}$ is the fully normalized Legendre function, a_{mn} and b_{mn} are the SH coefficients, α^i and z^i are the azimuth and zenith angles in the AF.

The SH coefficients are determined by constrained LSQ adjustment. Afterwards, the PCCs of the AUT are calculated for the entire antenna hemisphere according to Equation (4), transformed to PCO/PVC, and exported to IGS ANTEX (ANTenna EXchange) format.

For an in-depth description of the antenna calibration methodology at LMMT an interest reader is referred to Tupek et al. [14].

2.3. Antenna Calibration System at LMMT

The GNSS receiver antenna calibration system developed at LMMT consists of two major parts: hardware and software. Hardware-wise the calibration system consists of a

6-axis industrial robot Mitsubishi MELFA RV-4FLM-Q with its corresponding controller Mitsubishi MELFA CR750, two GNSS receivers (Trimble NetR5) and antennas, and a personal computer. An on-site calibration set-up at LMMT is depicted in Figure 2. The in-house custom-made software components of the calibration system, all written in Python, are the antenna calibration module (ACM), time synchronization module (TISY), and the PCC estimation module. An in-depth description of the calibration system operation can be found in Tupek et al. [14].
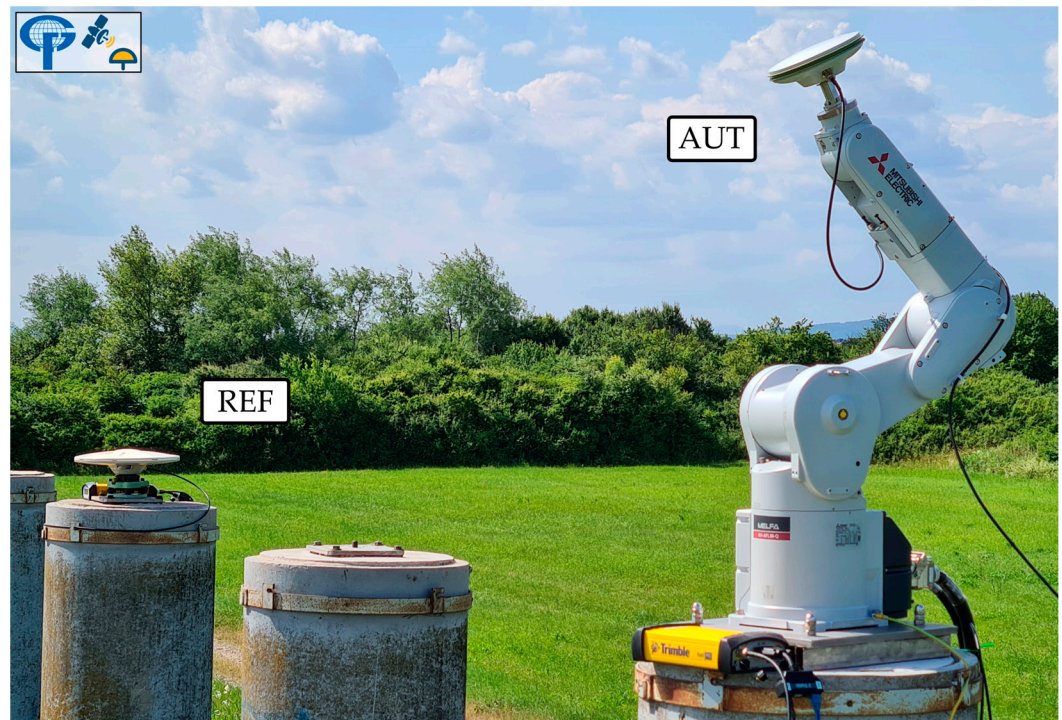
Figure 2. GNSS antenna calibration system at the Laboratory for Measurements and Measuring Technique (LMMT) of the Faculty of Geodesy of the University of Zagreb in Croatia; REF—Reference Antenna (TRM57971.00 NONE); AUT—Antenna-under-Test (LEIAX1202GG NONE). The calibration field consists of two 5-m-spaced pillars which are part of the Calibration Baseline of the Faculty of Geodesy of the University of Zagreb [17].

3. Results and Discussion

To test the antenna calibration system at LMMT and to validate the calibration results with Geo++ GmbH, an IGS approved calibration institution, from April to June of 2023 four calibration campaigns of the same GNSS antenna Trimble Zephyr 2 Geodetic (TRM57971.00 NONE, S/N: 30739001) for the GPS L1 frequency have been conducted. Figure 3 visualizes the main benefit of using a robot for antenna calibration, i.e., a full coverage of the entire antenna hemisphere, even after only approx. 2 h of calibration.
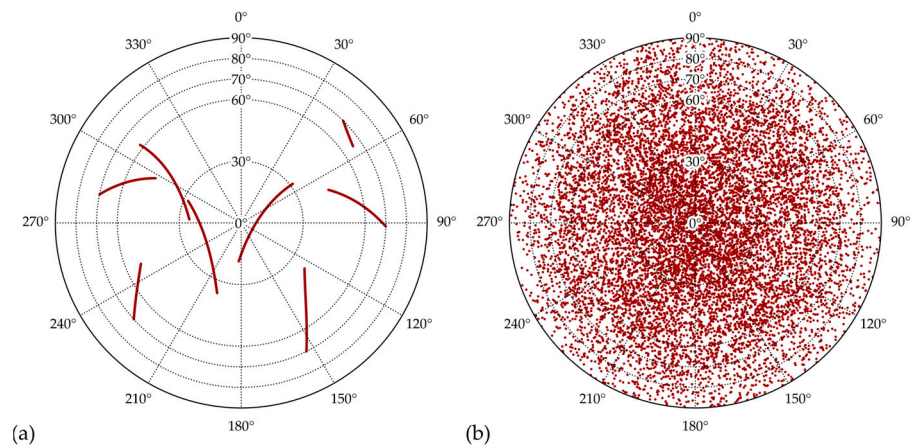
Figure 3. Satellite azimuth and zenith angle plot (sky-plot) during antenna calibration at LMMT; (**a**) topocentric frame (TF); (**b**) antenna frame (AF).

To validate the LMMT antenna calibration results, a comparison with an independent calibration has been conducted. For that purpose, the investigated antenna has been individually calibrated by Geo++ GmbH, an IGS approved institution, on 5 August 2022.

According to the new calibration method at LMMT, PCCs have been estimated for every conducted antenna calibration campaign. Lastly, to obtain a final solution, calibration results have been averaged, and the final PCO and PVC grid exported to ANTEX. Table 1 summarizes the LMMT and Geo++ GmbH estimated PCOs. The PCO differences between the LMMT and Geo++ GmbH calibrations are on the sub-millimeter level. The PCVs of the investigated antenna for the GPS L1 frequency, per calibration institution, are depicted in Figure 4. Both individual calibration results show similar PCV behavior over the entire antenna hemisphere, with noticeable larger values at the antenna horizon for the Geo++ calibrations. Also, for both calibration results (LMMT and Geo++ GmbH) small azimuthal variations are noticeable.

Table 1. PCO vector components of antenna TRM57971.00 NONE (S/N: 30739001) of GPS L1 (G01) frequency per calibration institution. All values are in millimeters (mm).

Calibration	Phase Center Offset (PCO)		
Institution	North	East	Up
Geo++ GmbH	0.79	0.32	66.96
LMMT	1.24	0.11	67.24
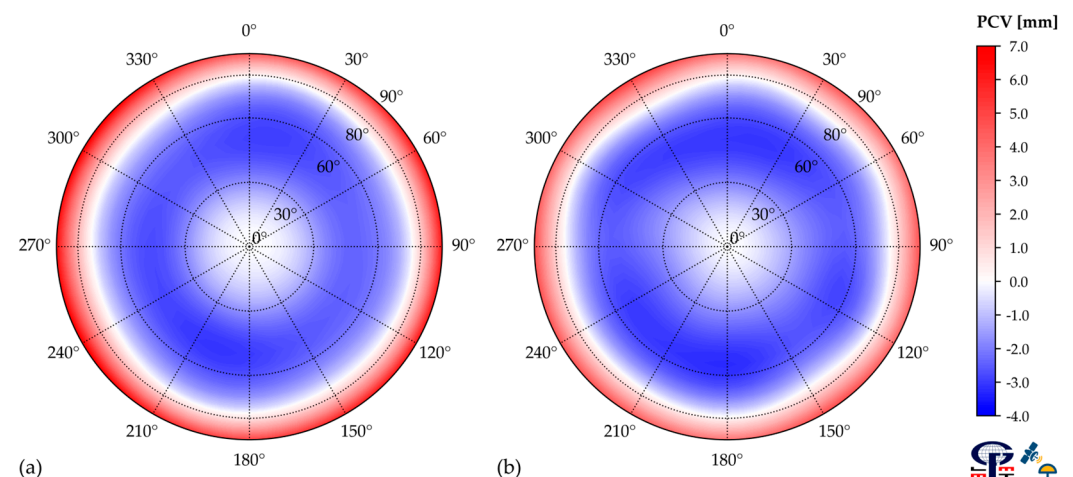
Figure 4. (**a**) Geo++ GmbH and (**b**) LMMT phase center variations (PCVs) of antenna TRM57971.00 NONE (S/N: 30739001) for GPS L1 (G01) frequency.

To estimate the accuracy of LMMT individual antenna calibration results, the Geo++ GmbH calibration results are taken as reference values. The PCC differences ΔPCC of antenna TRM57971.00 NONE (S/N: 30739001) for GPS L1 (G01) frequency, over the entire antenna hemisphere, are calculated and depicted in Figure 5. By simple visualization of the gained difference pattern, it is evident that values around zero prevail with larger values mainly located at low antenna elevations, e.g., for azimuth approx. 300°.

To obtain an quantitative accuracy estimation of LMMT calibration results, the following scalar measures of the PCC difference pattern are calculated: minimum and maximum ΔPCC, root-mean-square (RMS) deviation of ΔPCC, range of the ΔPCC, and the interquartile range (IQR) of the ΔPCC. All calculated values are given in Table 2. Furthermore, because during the majority of GNSS applications, a standard elevation mask of minimum 10° is used, a 10° elevation-reduced antenna hemisphere analysis is justified. All accuracy measures are determined accordingly and given in Table 2.
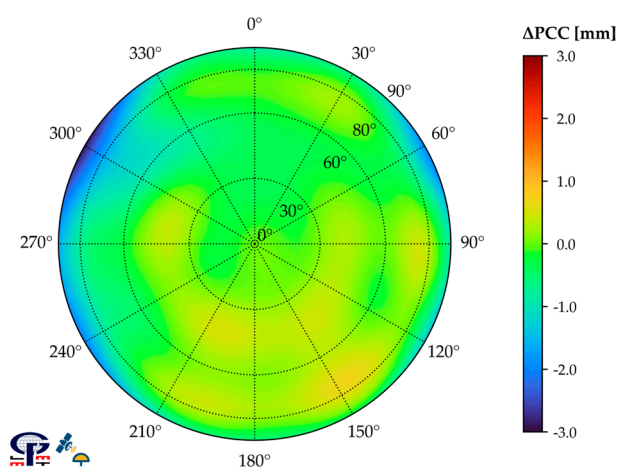
Figure 5. Geo++ GmbH and LMMT PCC differences (ΔPCC) of antenna TRM57971.00 NONE (S/N: 30739001) for GPS L1 (G01) frequency after transformation to common PCO and datum.

Table 2. Quantitative measures of the difference between Geo++ GmbH and LMMT individual absolute calibrations: minimum, maximum, root-mean-square (RMS) deviation, range, and interquartile range of ΔPCC. All values are in millimeters (mm).

Full Antenna Hemisphere (0° Elevation Cut-Off)					Reduced Antenna Hemisphere (10° Elevation Cut-Off)				
Min.	Max.	RMS	Range	IQR	Min.	Max.	RMS	Range	IQR
−2.92	0.72	0.52	3.64	0.44	−1.64	0.72	0.34	2.36	0.41

Considering the full antenna hemisphere, the LMMT and Geo++ GmbH PCC differences are in the interval from −2.92 to 0.72 mm, with the middle 50% of ΔPCC being within 0.44 mm. The RMS of the differences is 0.52 mm. However, if only the elevation-reduced antenna hemisphere is considered, accuracy measures significantly improve. The range of all ΔPCC is 2.36 mm with an RMS value of 0.34 mm whereby the middle 50% of the differences do not exceed 0.41 mm.

Therefore, to summarize, with the newly developed LMMT antenna calibration system an estimated agreement to accredited Geo++ GmbH calibrations to within 0.52 mm has been achieved.

4. Conclusions

The new GNSS receiver antenna calibration system developed at the at the Laboratory for Measurements and Measuring Technique (LMMT) of the Faculty of Geodesy of the University of Zagreb in Croatia, can provide meaningful antenna calibration results

for the GPS L1 frequency. From the gained experimental research results regarding the Trimble Zephyr 2 Geodetic antenna, an estimated agreement to within 0.52 mm, in term of RMS, with the accredited Geo++ GmbH results has been achieved. Therefore, our calibration results also confirm the compatibility of LMMT GPS L1 calibrations with the IGS accredited Geo++ GmbH calibrations.

References

1. Maqsood, M.; Gao, S.; Montenbruck, O. Antennas. In *Springer Handbook of Global Navigation Satellite Systems*; Teunissen, J.G.P., Montenbruck, O., Eds.; Springer International Publishing: Cham, Switzerland, 2017; pp. 505–534.
2. Wübbena, G.; Schmitz, M.; Menge, F.; Seeber, G.; Völksen, C. A New Approach for Field Calibration of Absolute GPS Antenna Phase Center Variations. *Navigation* **1997**, *44*, 247–255. https://doi.org/10.1002/j.2161-4296.1997.tb02346.x.
3. Wübbena, G.; Schmitz, M.; Menge, F.; Böder, V.; Seeber, G. Automated Absolute Field Calibration of GPS Antennas in Real-Time. In Proceedings of the 13th International Technical Meeting of the Satellite Division of The Institute of Navigation (ION GPS 2000), Salt Lake City, UT, USA, 19–22 September 2000; The Institute of Navigation: 2000; pp. 2512–2522.
4. Kröger, J.; Kersten, T.; Breva, Y.; Schön, S. Multi-Frequency Multi-GNSS Receiver Antenna Calibration at IfE: Concept-Calibration Results-Validation. *Adv. Space Res.* **2021**, *68*, 4932–4947. https://doi.org/10.1016/j.asr.2021.01.029.
5. Wübbena, G.; Schmitz, M.; Warneke, A. Geo++ Absolute Multi-Frequency GNSS Antenna Calibration. In Proceedings of the EUREF Analysis Centres Workshop, Warsaw, Poland, 16–17 October 2019.
6. Kröger, J.; Kersten, T.; Breva, Y.; Schön, S. Multi-GNSS Receiver Antenna Calibration. In Proceedings of the FIG Working Week 2020, International Federation of Surveyors, Amsterdam, The Netherlands, 10–14 May 2020; pp. 1–13.
7. Riddell, A.; Moore, M.; Hu, G. Geoscience Australia's GNSS Antenna Calibration Facility: Initial Results. In Proceedings of the International GNSS Society Symposium (IGNSS 2015), Gold Coast, Australia, 16–17 July 2015; pp. 1–12.
8. Bilich, A.; Erickson, B.; Geoghegan, C. 6-Axis Robot for Absolute Antenna Calibration at the US National Geodetic Survey. In Proceedings of the IGS Workshop 2018, International GNSS Service, Wuhan, China, 2018.
9. Hu, Z.; Cai, H.; Jiao, W.; Zhou, R.; Zhai, Q.; Liu, X.; Kan, H.; Zhao, Q. Preliminary Results of IGMAS BDS/GNSS Absolute Antenna Phase Center Field Calibration. In Proceedings of the China Satellite Navigation Conference (CSNC 2022), Beijing, China, 22–25 May 2022; Yang, C., Xie, J., Eds.; Springer: Singapore, 2022; pp. 147–160.
10. Willi, D.; Lutz, S.; Brockmann, E.; Rothacher, M. Absolute Field Calibration for Multi-GNSS Receiver Antennas at ETH Zurich. *GPS Solut.* **2020**, *24*, 28. https://doi.org/10.1007/s10291-019-0941-0.
11. Sutyagin, I.; Tatarnikov, D. Absolute Robotic GNSS Antenna Calibrations in Open Field Environment. *GPS Solut.* **2020**, *24*, 92. https://doi.org/10.1007/s10291-020-00999-8.
12. Dawidowicz, K.; Rapiński, J.; Śmieja, M.; Wielgosz, P.; Kwaśniak, D.; Jarmołowski, W.; Grzegory, T.; Tomaszewski, D.; Janicka, J.; Gołaszewski, P.; et al. Preliminary Results of an Astri/UWM EGNSS Receiver Antenna Calibration Facility. *Sensors* **2021**, *21*, 4639. https://doi.org/10.3390/s21144639.
13. IGS Antenna Working Group. Available online: https://igs.org/wg/antenna/#files (accessed on 1 August 2023).

14. Tupek, A.; Zrinjski, M.; Švaco, M.; Barković, Đ. GNSS Receiver Antenna Absolute Field Calibration System Development: Testing and Preliminary Results. *Remote Sens.* **2023**, *15*, 4622. https://doi.org/10.3390/rs15184622.
15. Hauschild, A. Combinations of Observations. In *Springer Handbook of Global Navigation Satellite Systems*; Teunissen, J.G.P., Montenbruck, O., Eds.; Springer International Publishing: Cham, Switzerland, 2017; pp. 583–604.
16. Hauschild, A. Basic Observation Equations. In *Springer Handbook of Global Navigation Satellite Systems*; Teunissen, J.G.P., Montenbruck, O., Eds.; Springer International Publishing: Cham, Switzerland, 2017; pp. 561–582.
17. Zrinjski, M.; Barković, Đ.; Špoljar, K. Review of Precise Calibration Methods of Geodetic Calibration Baselines. *Geod. List.* **2022**, *76*, 25–52.